Stiffness Analysis of a Class of Parallel Mechanisms for Micro-Positioning Applications

Hemanth K. Arumugam, Richard M. Voyles, Sanika Bapat
Department of Computer Science and Engineering
University of Minnesota
Minneapolis, MN 55455
hemanth@cs.umn.edu, voyles@cs.umn.edu, sanika@ece.umn.edu

***Abstract*—Micro-Positioning devices are increasingly being made of parallel manipulators due to their superior stiffness characteristics. This paper explores a variant of the classical six degrees-of-freedom Stewart-Gough Platforms for use in Micro-Positioning applications. Stiffness values of both these mechanisms are computed and compared for relative gain in theoretical stiffness achieved. An over-sized version of the platform was built for educational purposes.**

Keywords-parallel manipulators; stiffness; Jacobian; Stewart-Gough platform

I. INTRODUCTION

Parallel Mechanisms are increasingly being used to construct multi-axis micro-positioning devices due to their superior stiffness characteristics when compared to serial mechanisms. In addition, the errors in individual chains of a parallel manipulator do not directly sum to yield the overall manipulator positioning error. Hence when six linear actuators with a positioning error of 50nm are arranged serially the total end-effector positioning error could add up to as much as 300nm, whereas by arranging them in parallel will give an error of 50nm or less, neglecting other joint inaccuracies. But this increased overall positioning accuracy comes at the cost of a reduced workspace.

The overall stiffness and workspace of parallel mechanisms vary based on the way the parallel links are assembled together. In fact, there is always a tradeoff between stiffness and workspace in the configuration of such mechanisms. The family of parallel mechanisms based on Stewart-Gough Platforms is increasingly being used to construct micro-positioning devices. This paper explores the use of a specific variant of Stewart-Gough Platform made of PSS-chains for such an application. The rest of the paper is organized as follows: Section II discusses the basic structure of PSS-variants of the Stewart-Gough Platform. The stiffness calculations for the two forms of the platform are presented in Section III and Section IV. Section V presents the implications of using the PSS-variant for a micro-positioning device.

II. STEWART-GOUGH PLATFORMS

Stewart-Gough Platforms [3][4] are six-degrees-of-freedom parallel manipulators that are known for their high stiffness and limited workspace characteristics. In its most common form (Figure 1) it consists of a moving platform (end-effector) connected to a fixed platform (ground) by means of six Spherical-Prismatic-Spherical (SPS) links with the prismatic joint being actively controlled by a linear actuator. Many variants of the Stewart Platforms have been proposed, each having different platform configurations with respect to the number of points in the moving and fixed platforms to which these six SPS links are connected. A comprehensive review of these different configurations is presented in [2].

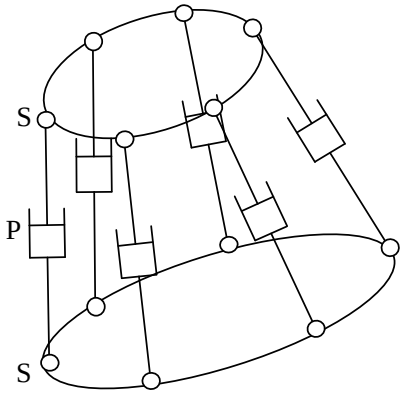

Figure 1. A General SPS 6-6 Stewart-Gough Platform.

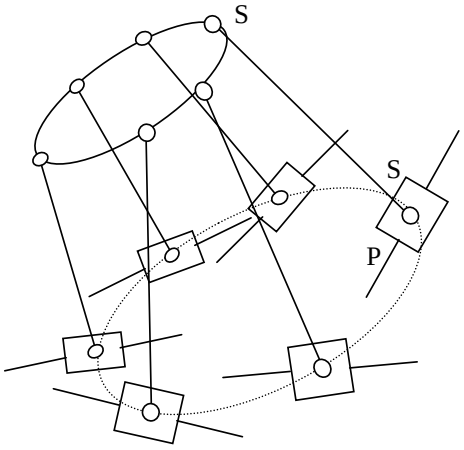

Figure 2. PSS variant of the Classical 6-6 Stewart-Gough Platform with arbitrary prismatic joint orientation.

One variant of the Stewart-Gough Platform arises by replacing each of the six SPS links with a PSS link with the prismatic joint being actively controlled as before. This is shown in Figure 2. Since the prismatic joints are now between the fixed platform and a PSS link member, this configuration gives rise to a stiffer manipulator, with implications on the size and shape of the end-effector workspace. Each of the prismatic joints can be oriented along any direction in space to achieve different stiffness and workspace characteristics. Specific variants of PSS 6-6 Stewart Platforms arise by orienting these prismatic joints along one of the three major axes.

III. STIFFNESS COMPARISON

In this section the Stiffness properties of SPS and PSS 6-6 Stewart-Gough platforms are computed. Their stiffness matrices can then be compared to understand the amount of stiffness gained by converting a SPS chain to a PSS chain. This can be done by treating the prismatic joints as the only source of compliance. Finally the effect of the orientation of these prismatic joints on the overall manipulator stiffness can be determined.

Although many sources of compliance contribute to the ultimate stiffness of the mechanism, we restrict our attention to the dominant source, the compliance of the prismatic joint along the axis of motion. This assumption is reasonably accurate if suitable pre-loads are applied to eliminate backlash.

A. Stiffness of a 6 DOF Manipulator

Stiffness Analysis can be posed as the problem of studying the effect of applied or external forces, **F**, on the compliance of the end-effector as a whole

$$\mathbf{F} = \mathbf{K}\,\Delta\mathbf{x} \tag{1}$$

where $\Delta\mathbf{x}$ is the end-effector deflection and **K** is the overall stiffness matrix of the manipulator.

Let **f** = [f1, f2, … f6] be the vector of actuated forces acting on the six prismatic joints. Using the Principle of Virtual Work it can be shown that [1] for the manipulator to be in static equilibrium, the external forces **F** is related to the actuator forces **f** by the Jacobian,

$$\mathbf{F} = \mathbf{J}^{T}\mathbf{f} \tag{2}$$

Assuming that the only sources of compliance are due to the six prismatic joints, the individual joint displacements $\Delta\mathbf{e}$ = [e1, e2,… e6], can be related to the end-effector compliance $\Delta\mathbf{x}$ by the Kinematic Jacobian,

$$\Delta\mathbf{e} = \mathbf{J}\,\Delta\mathbf{x} \tag{3}$$

But each actuator i, has its stiffness ki defined by

$$\mathrm{fi} = \mathrm{ki}\ \mathrm{ei} \tag{4}$$

Now from all of the above equations the overall manipulator stiffness K can be obtained[1] as

$$\mathbf{K} = \mathbf{J}^{T}\,\mathrm{diag}[\mathrm{ki}]\,\mathbf{J} \tag{5}$$

If each of the actuator is assumed to have same stiffness, k, the overall stiffness matrix reduces to

$$\mathbf{K} = \mathrm{k}\,\mathbf{J}^{T}\mathbf{J} \tag{6}$$

Thus the overall manipulator stiffness is dependent on the kinematic jacobian which is in turn dependent on the pose of the manipulator.

B. Stiffness of a 6-6 SPS Stewart-Gough Platform

Stiffness of a general 6-6 Stewart-Gough Platform has been extensively studied [1][2][5]. The overall manipulator stiffness for a SPS-platform is derived as follows,

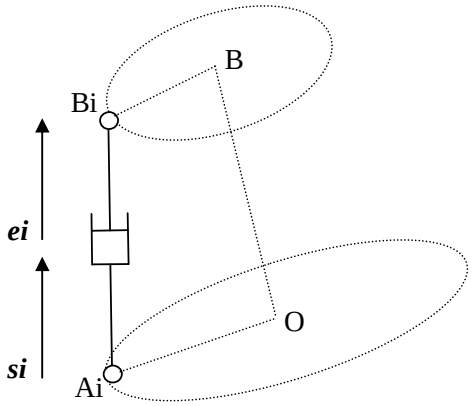

Figure 3. A leg of SPS 6-6 Stewart-Gough Platform.

Let **ai** and **bi** denote the vectors of locations where the six legs are connected to the ground plane and end-effector respectively. Let $\mathbf{V}_B = [\mathbf{v}_B^{\ T}\ \boldsymbol{\omega}_B^{\ T}]^T$ denote the velocity of the moving platform. Let **V** = [v1, v2 … v6] be the linear velocity of the six actuators and ***si*** be the *unit vector* along the ith SPS link. First the kinematic jacobian of the platform is computed using a procedure described in [1].

From Figure 3, the loop-closure equation for each leg of the manipulator can be written as,

$$\mathbf{OB} + \mathbf{BB_i} = \mathbf{A_iB_i} + \mathbf{OA_i} \tag{7}$$

Differentiating the above equation with respect to time and dot-multiplying both sides by ***si*** gives,

$$\boldsymbol{si}\ .\ \mathbf{v}_B + (\mathbf{bi} \times \boldsymbol{si}).\boldsymbol{\omega}_B = \mathrm{vi} \tag{8}$$

Rewriting the above equation for each leg, results in

$$\mathbf{J_x}\,\mathbf{V}_B = \mathbf{J_e}\,\mathbf{V} \tag{9}$$

where $\mathbf{J_x} = [\boldsymbol{si}^{\,T}\ (\mathbf{bi} \times \boldsymbol{si})^T]$ and $\mathbf{J_e} = \mathbf{I}_{6x6}$

The kinematic Jacobian can then be computed using the relation,

$$\mathbf{J} = \mathbf{J_e}^{-1}\,\mathbf{J_x} \qquad (10)$$

The above equation can be used to compute the stiffness of the general Stewart platform using equation (6).

C. *Stiffness of 6-6 PSS Stewart-Gough Platform*

Kinematic Jacobian of a 6-6 PSS Stewart-Gough Platform can be computed in a similar way. From Figure 4, the loop-closure equation for each PSS leg can be written as,

$$\mathbf{OB} + \mathbf{BB_i} = \mathbf{A_iB_i} + \mathbf{OA_i} \qquad (11)$$

Expanding $\mathbf{OA_i}$ in terms of the actuator displacement $\mathbf{O_iA_i}$ leads to,

$$\mathbf{OB} + \mathbf{BB_i} = \mathbf{A_iB_i} + \mathbf{OO_i} + \mathbf{O_iA_i} \qquad (12)$$

Differentiating the above equation with respect to time and dot-multiplying both sides by ***si*** gives

$$\boldsymbol{si} \cdot \mathbf{v}_B + (\mathbf{bi} \times \boldsymbol{si}).\boldsymbol{\omega}_B = \text{vi}\ \boldsymbol{ei}.\boldsymbol{si} \qquad (13)$$

where ***ei*** is a *unit vector* along the ith actuator. Note that in a PSS configuration ***ei*** and ***si*** are different. Rearranging the above equation in terms of $\mathbf{J_x}$ and $\mathbf{J_e}$ as before

$$\mathbf{J_x}\,\mathbf{V}_B = \mathbf{J_e}\,\mathbf{V} \qquad (14)$$

where $\mathbf{J_x} = [\boldsymbol{si}^{\,T}\,(\mathbf{bi} \times \boldsymbol{si})^T]$ and $\mathbf{J_e} = \text{diag}[\boldsymbol{ei}.\boldsymbol{si}]$

The above result together with equation (6) can be used to compute the stiffness of 6-6 PSS Stewart-Gough Platform.

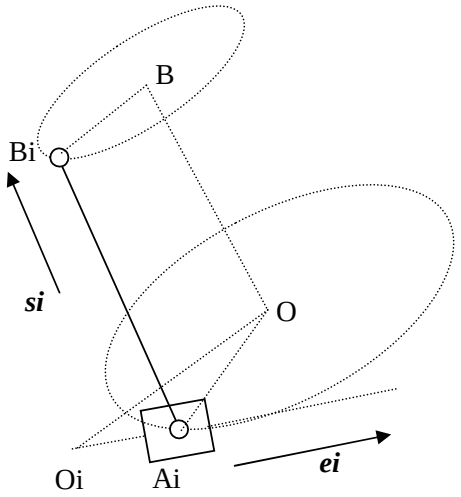

Figure 4. A leg of PSS 6-6 Platform.

Note the difference in the value of $\mathbf{J_e}$ between PSS and SPS configuration. This forms the basis for choosing the orientation of the actuators ***ei*** that will maximize the stiffness of the PSS manipulator.

D. *Comparison of Stiffness Values*

Comparing $\mathbf{J_e}$ from equations (9) and (14) helps one to understand the effect of the SPS and PSS linkage on the manipulator stiffness. Note that since both ***ei*** and ***si*** are unit vectors, the value of each diagonal entry of $\mathbf{J_e}$ in equation (14) is between -1 and +1. This implies that $|\mathbf{J_e}^{PSS}| < |\mathbf{J_e}^{SPS}|$ or $\mathbf{K}^{PSS} > \mathbf{K}^{SPS}$. Thus, all things being equal, the effect of making SPS linkage into a PSS linkage will always result in a stiffer manipulator.

Ideally, one could design a manipulator of infinite stiffness by setting $\mathbf{J_e} = [0]$. This theoretical limit is achieved when $\boldsymbol{ei}.\boldsymbol{si} = 0$, i.e. the orientation of each manipulator leg is perpendicular to the axis of the translational actuator to which it is connected. Of course, this is a singular configuration as instantaneous actuator motion has no effect on the leg. In practice ***ei*** is fixed during design time and ***si*** depends on the instantaneous orientation of each leg. Alternatively, one could use the above fact as an optimization criterion to decide on the best possible orientation of the prismatic joints that maximizes the overall stiffness of the manipulator for a desired workspace.

E. *Stiffness at Home Position*

In the previous sections it is shown that all things being equal, a PSS-based platform has superior stiffness characteristics than a SPS or conventional Stewart-Gough Platform. For a PSS platform, the theoretical stiffness value has a minimum value equal to the stiffness of an equivalent SPS-platform and a maximum value of infinity. If the orientation of the prismatic joints, ***ei*** are given for a PSS-platform, then one can determine the maximum improvement in stiffness that can be achieved over normal working ranges for a platform. For sake of simplicity, 6-3 version of SPS and PSS platforms are compared at their home positions to compute the increase in stiffness. The plan view of the platforms compared is shown in Figure 5.

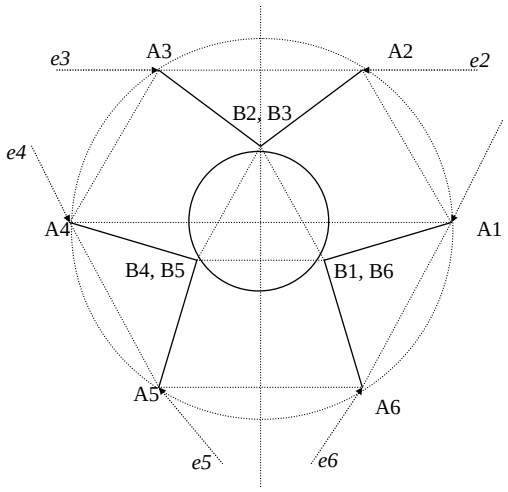

Figure 5. Plan View of an equivalent SPS and PSS Platform at Home.

Both the platforms have identical moving platform, B, of radius b and a fixed platform, A, of radius a. The top end of

each of the six legs is connected to the moving platform at locations Bi [i = 1 to 6] by an S joint. The bottom end of each of the six legs connects to the ground at locations Ai [i = 1 to 6] by means of an S or P joint respectively. While Ai remains fixed for a SPS-platform, the values of Ai shown in Figure 5 are true only at the home position for a PSS-platform. Also, the orientations of the six prismatic joints for the PSS- platform are fixed along vectors ***ei*** [i = 1 to 6] as shown in the figure. Finally, at the home position the end-effectors of both configurations are located at a height, h above the ground and have the same orientation as that of the ground reference frame.

It follows that ,

$$a1 = [a \quad , 0 \quad , 0]^T$$
$$a2 = [a/2 \quad , \sqrt{3}\, a/2 \quad , 0]^T$$
$$a3 = [-a/2 \quad , \sqrt{3}\, a/2 \quad , 0]^T$$
$$a4 = [-a \quad , 0 \quad , 0]^T$$
$$a5 = [-a/2 \quad , -\sqrt{3}\, a/2 \quad , 0]^T$$
$$a6 = [a/2 \quad , -\sqrt{3}\, a/2 \quad , 0]^T$$

$$b1 = b6 = [\sqrt{3}\, b/2 \quad , -b/2 \quad , h]^T$$
$$b2 = b3 = [0 \quad , b \quad , h]^T$$
$$b4 = b5 = [\sqrt{3}\, b/2 \quad , -b/2 \quad , h]^T$$

At home position, the length of each of the six legs is equal to d for both configurations. The following identity results by applying the loop-closure,

$$d^2 = a^2 + b^2 - \sqrt{3}ab + h^2$$

Using the above results in (16) it can be shown that,

$$\mathbf{J}_e^{PSS,\ home} = (-\ a/2d)\ \mathbf{I}_{6x6} \qquad (15)$$

Using (6), (9), (10) and (15) finally gives,

$$\mathbf{K}^{PSS,\ home} = (4d^2/a^2)\ \mathbf{K}^{SPS,\ home} \qquad (16)$$

Note that from $\Delta A6A1B1$, $2d > a$, or $\mathbf{K}^{PSS,\ home} > \mathbf{K}^{SPS,\ home}$ which verifies the results of Section D. More interestingly (16) relates the amount of stiffness gained by the platform as a function of the platform design parameters.

IV. Special Cases of PSS 6-6 Stewart-Gough Platform

The problem of arriving at an optimal set of values for the prismatic joint orientations, ***ei***, which minimizes the overall manipulator stiffness within its nominal workspace is an interesting one. However, manufacturing constraints would restrict the allowable values for ***ei***. Of particular relevance are the following two classifications of PSS 6-6 Stewart-Gough Platforms,

i. *Plane-Normal orientation*: when ***ei*** is [0,0,1]. All the actuators are oriented in vertical direction. See Figure 6(a).

ii. *In-Plane orientations*: when ***ei*** is [cos θ_i, sin θ_i, 0] where, θ_i is the orientation of the axis of the ith actuator with respected to global x-axis. All the actuators lie in xy plane. See Figure 6(b).

Both the platforms have superior stiffness values when compared to an equivalent SPS-platform, but have vastly different workspace shape. A Plane-Normal orientation of actuators would give rise to a manipulator that has an increased workspace in z-direction, and hence suited when workspace height is of importance. However, In-Plane orientations of the actuators will result in a family of manipulators that have a wide range of workspace configurations.

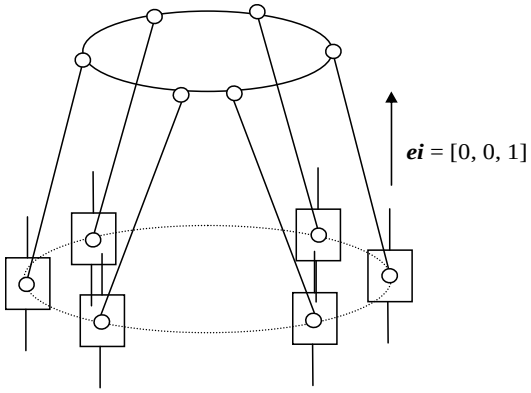

Figure 6 (a). PSS Platform where ei = z-axis

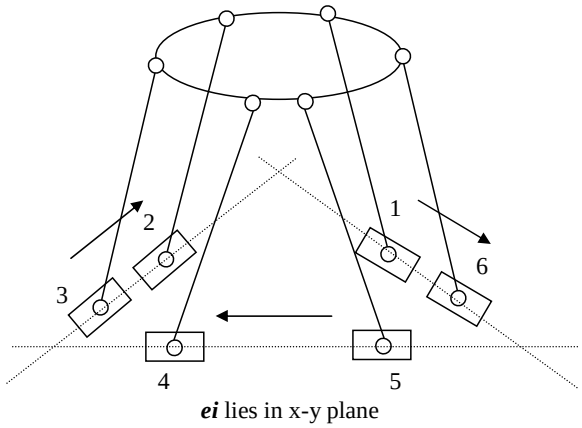

Figure 6 (b). PSS Platform where ei lies in x-y plane

V. Use in Photonics Assembly

The assembly of photonics devices is not often associated with large forces and high stiffness. After all, photons exert negligible forces and it is generally not necessary for photonic devices to come in contact. For example, aligning a photodiode with a micro ball lens involves positioning the photodiode at a focal point some distance from the lens. They do not come in contact.

Yet, in photonics assembly, potentially large forces can result when devices are immobilized. In the photodiode case above or, in the simplest case of aligning two optical fibers to form a coupling (not using a fusion bonder), one device would be affixed to a substrate with solder, UV epoxy, or welding, then the other device would be actively aligned to the first and similarly attached to the substrate. Considering a single-mode fiber-to-fiber coupling held together with solder pads of 500-micron diameter, the solder would shrink upon cooling to room temperature about 600 nanometers (assuming tin-lead solder). Four such solder balls would exert up to 13 N in pulling the aligned component down with it. Since single-mode optical fibers must be aligned to accuracies of a few tenths of a micron to maintain loss below 0.1 dB, the stiffness of the manipulator is of utmost importance.

Due to the superior stiffness characteristics of PSS 6-6 Stewart-Gough Platform, they are an ideal choice for high-frequency force-feedback applications like Photonics Assembly where the size of the workspace is negligible. Among the various possible PSS-platform configurations, a triangular layout of actuators in xy plane, shown in Figures 5 and 6(b), is of importance in micro-positioning applications due to the following properties,

i. Since the actuators are laid down and supported on the ground plane, they have higher stiffness when compared to a Plane-Normal orientation of the actuators.

ii. By laying out the slides in a triangular pattern, pairs of linear slides, 1-6, 2-3, 4-5 (see Figure 6(b)), could be aligned more accurately during construction or possibly built together during machining.

VI. Implementation

We have implemented a manipulator utilizing this basic design, but at a much different scale. The manipulator, illustrated below, was not implemented for micropositioning. Instead, it was built as a personal flight simulator for a laboratory class on real-time systems. While the scale is dramatically different, the proportions are the same as our micro-positioner, so we will use it as an over-sized model for verification of predicted results. This will allow us to build evidence in support of our design to pursue funding for the much greater cost associated with a sub-micron precision microassembly tool.

Our stiffness analysis assumed idealized conditions that are not achievable in practice. Although the analysis is valuable as a design approach for selecting a configuration, it will likely be highly inaccurate at the 50 nm scale. Our goal in building a device at this macro scale is to inexpensively develop a platform on which to study the secondary effects of non-ideal structures, transmissions, and bearings using conventional metrology. We will build and test models of flexibility and backlash in the actuators, torsional flexibilities in slides, and even friction models will be studied because of their profound importance in the sub-micron realm.

As an example, we gathered some accelerometer and proprioceptive data from the flight simulator. The proprioceptive data was gathered from encoders on each motor while a constant amplitude sine wave was commanded in the z direction in Cartesian space. The characteristic resonant spike appears in Figure 8 at about 12 rad/s for a zero-to-peak amplitude of 12 mm. However, Figure 9 is the same data at a zero-to-peak amplitude of 5 mm. Note the secondary resonant peaks

The accelerometer indicated the chair could exert one-half-g acceleration on an 85 kg rider with its current low-level control tuning.

Fig. 7. The over-sized robotic chair for teaching real-time systems.

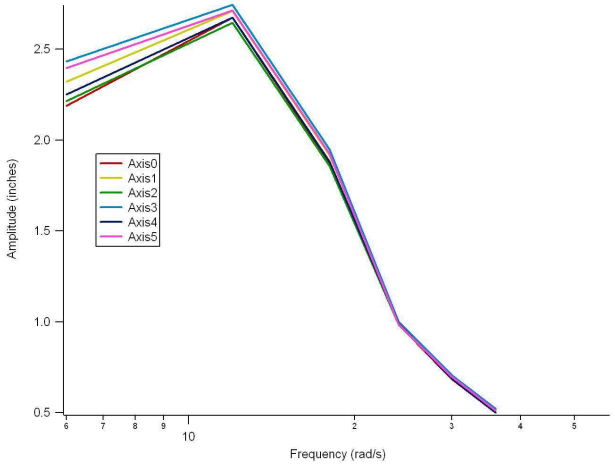

Fig 8. Frequency response of each of the six actuators with a zero-to-peak amplitude of 12 mm.

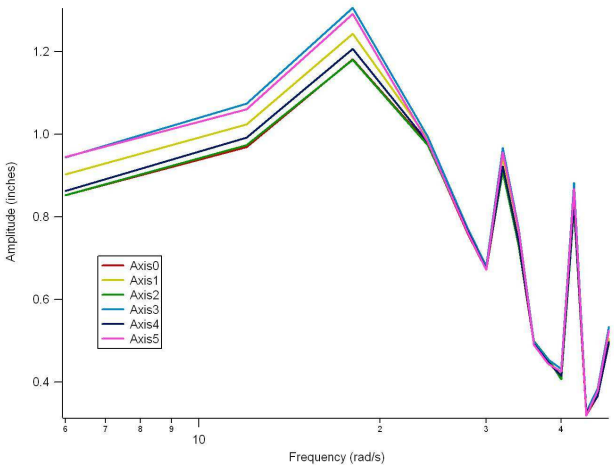

Fig 9. Frequency response of each of the six actuators with a zero-to-peak amplitude of 5 mm.

VII. CONCLUSIONS

PSS-variant of a 6-6 Stewart-Gough Platform is studied for its use as a Micro-Positioning device. Stiffness Analysis of the PSS-Platform is made. It is shown that the Stiffness of any configuration of PSS-platform is higher than a conventional SPS-platform, which makes it a good choice for Micro-Positioning Applications. There is an inherent tradeoff between stiffness and workspace of any manipulator when using this analysis methodology, but of the various design choices available for orienting the actuators of a PSS-platform, the Plane-Normal and In-Plane orientations are compared due to the ease in manufacturing such platforms.

VIII. ACKNOWLEDGEMENTS

We wish to thank Bradley Ferguson-Jarnes and Steven Damer for their control code and applications on the flight simulator as well as data gathering.

REFERENCES

[1] Lung-Wen Tsai, *Robot Analysis: The Mechanics of Serial and Parallel Manipulators*, John Wiley & Sons, 1999.

[2] Jean-Pierre Merlet, *Parallel Robots*, Kluwer Academic Publishers, 2000.

[3] V.E. Gough, and S.G. Whitehall, "Universal Tyre Test Machine", *Proceedings of the 9th International Techical Congress*, FISTIA, p.177, 1962.

[4] D. Stewart, "A Platform with Six Degrees of Freedom," *Proceedings of the Institute of Mechanical Engineers*, London, v.180, pp.371-386, 1965.

[5] C. Gosselin, "Stiffness Mapping for Parallel Manipulators", *IEEE Transactions on Robotics and Automation*, v.6, no.3, pp.377-382, 1990.